ALIGNMENT SYSTEM TESTS ON THE CERN REMOTE ALIGNMENT SYSTEM MOCK-UP

M. Sosin*, V. Barbarroux, Piotr Biedrawa [1], J. Calmels, M. Dandekar, J. Falcao Machado, R. Fernandez Bautista, C. Cala Franco, A. Herty, J. Kampp, W. Jasonek [1], H. Mainaud Durand, M. Noir, B. Pudlo [2] , V. Rude, P. Sarvade, CERN, Geneva, Switzerland
[1] also at AGH, University od Science and Technology, Krakow, Poland
[2] also at Politechnika Krakowska, Cracow University of Technology, Krakow, Poland

Abstract

The High Luminosity upgrade of the Large Hadron Collider (HL-LHC) aims to enable continuous operation at luminosities which are a factor of five above the LHC design value. To meet this goal, components installed in the Long Straight Sections around the ATLAS and CMS experiments must be aligned to within a tolerance of 0.17 mm vertically and 0.33 mm radially over a length of 420 meters. This precise alignment necessitated the development of a range of novel interferometric and capacitive sensor solutions, their acquisition systems, and micrometric resolution adjustment mechanics. This all falls under the scope of a new Full Remote Alignment System (FRAS) framework. To validate the FRAS sensors and adjustment mechanisms and confirm positioning strategies, a dedicated test bench known as the Single Component Test (SCT) was deployed at CERN. The SCT comprises a real LHC prototype magnet equipped with the full set of FRAS sensors and actuators, integrated into a tunnel-like configuration. This setup allows for the validation of all components under real operational conditions and serves as a rehearsal platform to cross-check the integration of all systems before their final deployment in the LHC tunnel.

This paper describes the SCT setup, the integration of FRAS systems, the tests conducted, and summarizes the test results and lessons learnt.

INTRODUCTION

The goal of the High Luminosity Large Hadron Collider (HL-LHC) project is to achieve a five times increase in the instantaneous collision rate and a ten times increase in the integrated luminosity compared to the nominal design values of the LHC [1]. To reach this objective, several key innovations that push accelerator technology beyond its current limits are planned, causing the need of replacement of nearly 1.2 km of the LHC beam lines with new components. Among these innovations are cutting-edge superconducting magnets, compact superconducting cavities, and other advanced technologies that will be mostly installed in the Long Straight Sections (LSS) around the ATLAS and CMS high luminosity experiments. These components must be aligned to a vertical accuracy of 0.17 mm and a radial accuracy of 0.33 mm over a length of 420 m [2]. To meet these alignment requirements while minimizing radiation exposure to personnel, a Full Remote Alignment System will be implemented. This system will facilitate remote position monitoring and adjustment of 76 HL-LHC beam line components installed in the tunnel. Each component will be equipped with alignment sensors to determine its position, and supported by motorized adjustment systems with micrometric resolution allowing for remote alignment within a transverse range of ±2.5 mm along the length of the LSS.

The accurate positioning of HL-LHC components in the tunnel will rely on high-precision sensors [2–5] that will be installed on each component to provide position monitoring with 5 or 6 Degrees of Freedom (DOF):

- Capacitive technology based Wire Positioning Sensors (WPS) for determining the vertical and radial positions of components (sensor accuracy < 5 µm);
- Frequency Sweeping Interferometry (FSI) based Hydrostatic Levelling Sensors (HLS), for determining vertical positions (sensor accuracy < 5 µm);
- Capacitive and FSI-based inclinometers for roll angle determination (sensor precision < 15 µrad; sensor accuracy: absolute angle measurement with respect to sensor interface < 150 µrad);
- FSI longitudinal monitoring sensors for determining the longitudinal position of components (sensor accuracy < 10 µm);
- Special optical vacuum heads (feedthroughs) and cryogenic reflectors for measuring the distance between the cryostat vacuum head situated at room temperature and the cold component within the cryostat that hold the reflectors at cryogenic temperatures (sensor accuracy < 10 µm).

For the remote adjustment of HL-LHC component positions in the tunnel, two solutions will be used: the Universal Adjustment Platform (UAP) for components weighing less than 2 tons and motorized jacks for components above 2 tons [2, 3, 6]. These systems will allow the component adjustment in 5 DOF (the longitudinal direction will not be remotely adjusted, as it is considered non-critical for accelerator performance [2]).

All sensor data acquisition and actuator motion commands will be managed using CERN-developed electronics. Real-time control will be provided by Linux Front-End Computers

* mateusz.sosin@cern.ch

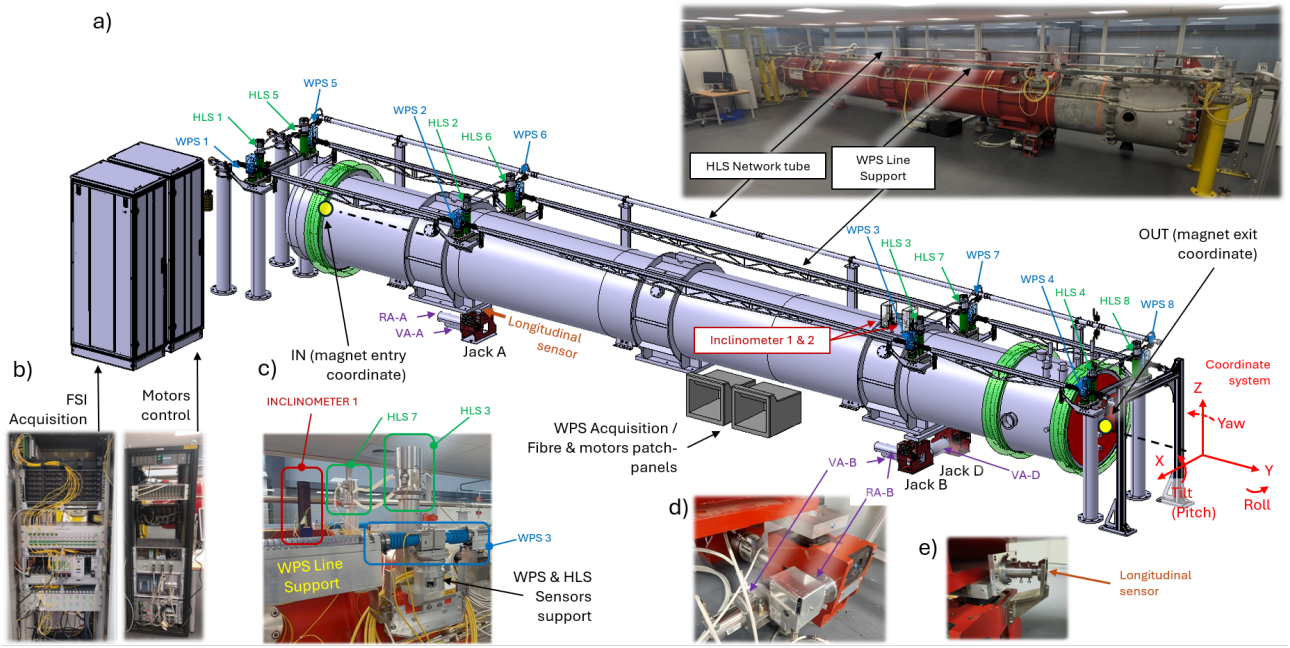

Figure 1: SCT mock-up with FRAS sub-components: a) picture taken after commissioning and 3D model of SCT mock-up; b) FSI and Motor control racks; c) WPS/HLS sensor support and integration of WPS Line support; c) HL-LHC jack equipped with vertical and radial adapter (VA, RA).

(FECs) operating within the CERN Front-End System Architecture (FESA) framework [7], with operator supervision through the CERN UNified Industrial COntrol System (UNICOS) [8], based on the SIEMENS WinCC OA Supervisory Control And Data Acquisition (SCADA) system.

Given the scale of the FRAS system and the number of new technologies involved, a comprehensive qualification strategy has been implemented to mitigate the risks associated with deploying new solutions. This strategy consists of three main stages:

- Stage 1 (2016-2023): Focused on the individual qualification of all types of sensors, their supports, and motor assemblies.
- Stage 2 (Started in 2023): Focused on validating the full strategy on a single accelerator component, at ambient temperature, in what is called the Single Component Test (SCT).
- Stage 3 (foreseen between 2024-2026): Validation on the IT String Test facility, consisting of six full-scale and interconnected HL-LHC magnets. This will allow a check of FRAS installation procedures, building on the SCT experience, and will test all FRAS systems on six magnets under nominal, cold conditions.

This paper details the tests conducted on the SCT mock-up during Stage 2. It summarises the results obtained and discusses the lessons learnt.

SINGLE COMPONENT TEST MOCK-UP

To perform an initial validation of the entire FRAS strategy, it was decided to equip a real magnet with a representative set of FRAS systems, including sensors, actuators, acquisition units and controls. These systems were integrated in a way that reflects the most complex HL-LHC instrumentation configuration. The SCT mock-up allowed the component installation ergonomics to be validated, the operational performance to be checked, and the combined testing of all FRAS sub-components (both hardware and software) under dynamic (motion) conditions.

Figure 1 shows the layout of the SCT and provides images of the real implementation of its sub-components. The mock-up is based on an old LHC prototype quadrupole with an approximate weight of 20 tons, known as the Twin Aperture Prototype (TAP). The TAP is equipped with a redundant sensor configuration, mirroring the double-wire setup of the HL-LHC inner triplet section of FRAS, consisting of:

- 8 capacitive WPS sensors: 4 (WPS 2, 3, 6, 7) are installed on the TAP magnet (which moves with the component), and the other 4 (WPS 1, 4, 5, 8) are installed on external reference pillars (fixed to the ground). Two separate wires are stretched between two pairs of extremity pillars on each side of the component.
- 8 FSI-HLS sensors: 4 (HLS 2, 3, 6, 7) are installed on the TAP magnet (moving with the component), and the other 4 (HLS 1, 4, 5, 8) are installed on external reference pillars (fixed to the ground). All HLS sensors are connected to an HLS Network Tube using flexible

silicon tubes, providing a common water level in the sensors.

- 2 FSI-inclinometers installed on top of the TAP, providing roll angle measurements of the component.
- Longitudinal FSI-based sensor for monitoring the longitudinal (Y-direction, Fig.1.a) position.
- The external reference pillars were equipped with vertical FSI measurements sensors, to monitor the thermal expansion of these reference pillars.

The TAP is supported by three motorized HL-LHC jacks (A, B, D in Fig.1.a), to perform the remote adjustment of the TAP in 5 DOF. Jacks A and B are equipped with vertical and radial adapters (VA, RA), while jack D is equipped only with a vertical adapter, as the longitudinal adjustment provided by jack D is manual.

Acquisition and control units are distributed across three separate racks:

- The FSI Interferometer rack, which houses all optical circuits, photodetector electronics, and a dedicated high-throughput Graphics Processing Unit (GPU) based server for real-time data processing.
- The Motor control rack, which includes the Sensors Acquisition and Motion Control system (SAMbuCa) [9] electronics and stepper motor drivers.
- The WPS sensor acquisition sub-rack, located below the TAP magnet.

TESTS AND RESULTS

Validation of FRAS sub-component integration, installation procedures and measurement network routing

The installation of the components and associated measurement networks was the first stage of SCT testing, aiming to validate installation procedures and verify the stability of mechanical supports after installation. The following installation steps were reviewed and provided immediate feedback for design and procedural adjustments:

- HLS Network tube installation and height levelling: This step involved installing the HLS network tube and its supports, followed by a maximum deformation (stiffness) check under lateral disturbing forces.
  The test confirmed the correct design of the adjustment mechanisms, but also prompted minor updates to the supports to increase their rigidity in the transverse direction.
- Jack installation (see Fig.1.a,d): This process included marking the floor, drilling holes, pre-adjusting the jacks, positioning them on the floor, and securing them. Following the installation, the TAP magnet was placed on the jacks and manually pre-adjusted to its nominal position.
  No significant issues or obstacles were encountered during this stage.
- Extremity pillar installation (see Fig.1.a): This step involved marking the floor, drilling holes, and pre-adjusting the pillar positions before securing them.
  The test led to a revision of the approach for verticalizing the pillars, resulting in design adjustments to the shims and updates to the installation procedure.
- Installation of WPS and HLS Sensor supports and other supporting plates (see Fig.1.c): The supports were installed on the magnet interfaces and their height and tilt pre-adjusted. After installation, the stability of the WPS and HLS supports under lateral disturbing forces was compared with initial lab test results. This test was crucial because the stability of the WPS and HLS supports directly affects the accuracy of component position determination. The supports must remain rigid after height and tilt pre-adjustment, and their top surfaces must remain stable after disturbances simulating possible tunnel scenarios (e.g. accidental pulling by personnel).
  The test confirmed the initial lab results that the support top surfaces remained stable after pre-adjustment and under lateral disturbing forces (up to approximately 40 kg), validating the proper design of the supports and their mounting method on the magnet interface.
- WPS Line support installation and stiffness validation: During the installation of the WPS Line support, difficulties arose in adjusting the height properly, due to issues with welding deformations and unexpectedly low transverse stiffness (which had been assessed as sufficient during design simulations).
  Practical verification on the SCT indicated the need for a redesign: the original welded, truss-reinforced design (see Fig.1.a) was replaced with an extruded aluminium profile, as seen in Fig.1.c. This redesign also resolved an issue with fibre routing, which is discussed later.
- Cable and fibre network routing: FRAS requires the installation of a large number of cables and fibres between the patch panel (installed below the component to be aligned) and the sensors and motors. This test provided the first practical exercise in routing these networks in an environment similar to the tunnel.
  The test confirmed that the cable tray solution (fixed along the magnet) was sufficient for cables but not suitable for fibres. Even reinforced fibres are fragile and difficult to re-route in case of need. Consequently, the decision was taken to separate the fibre routing from the cable routing and update the installation procedure. A new fibre routing duct was integrated within the extruded profile of the WPS Line support, which also improved the transverse stiffness of the profile. Additionally, a special set of fibre duct termination connectors

was designed to facilitate a smooth transition between the WPS Line support profile and the fibre protection tubes, delivering fibres directly to the sensors.

After the installation and adjustment of all mechanical components, the sensor interfaces located on their supports were fiducialised. The coordinates of these interfaces were measured using a laser tracker. The sensor interfaces were fiducialised with an accuracy of 25 µm with respect to the TAP reference frame. These data were registered in relevant configuration databases, enabling future accurate position determination using the sensors.

SCT system commissioning and the role of the mock-up as a control system rehearsal platform

The commissioning phase was initiated once the sensors were installed on their supports. The first step was to cross-check the connections between sensors, motors, and electronic channels against the mapping tables designed for control system objects' instantiation. After verifying these connections, the WPS sensors were calibrated. This calibration was necessary because the capacitive technology used in these sensors requires the entire measurement chain — including the sensor, cable, and conditioning electronics — to be calibrated.

Once the connections were verified and the necessary calibrations completed, final commissioning of the sensors was carried out using a basic version of the FRAS control software [11]. This allowed the validation of logical connections between hardware and software channels and the debugging of basic software blocks for sensors, motors, and acquisition systems. From this point onward, sensor measurements were registered in CERN's data logging database, NXCALS [12].

With all the sensor data now continuously logged, we were able to validate the consistency of all previously collected data, such as geodetic network measurements and the fiducialization and sensor calibration. This was done by applying external least squares adjustment scripts and checking the sensor measurement residuals and quality parameters of the SCT least squares adjustment model estimator. The maximum residuals were: for WPS sensors 6 µm; for HLS 21 µm; for inclinometers 96 µrad and 55 µm for longitudinal sensors. The accuracies for the TAP magnet DOF position estimation were (cf. Fig.1): 21 µm in X (radial), 18 µm in Z (vertical) and 148 µm in Y (longitudinal) directions; and for rotations: 2 µrad in pitch, 19 µrad in roll and 3 µrad in yaw angle determination.

It is important to note that at this stage the SCT became the primary platform for rehearsing all future control system developments. The availability of sensors and motors allowed for continuous testing and upgrades of the remaining FRAS software blocks, a process that is still ongoing.

FSI-HLS dynamic response tests

After commissioning the SCT with operational FSI-HLS sensors, one of the first aspects to be examined was the behaviour of FSI measurements under dynamic conditions. FSI measurements are sensitive to vibrations [13], meaning that water motion or waves on the water surface can affect the precision of HLS measurements. Knowing this limitation, the primary objective of the test was to assess how typical FRAS (TAP) component motion scenarios would impact measurements. The secondary objective was to verify how potential disturbance scenarios, such as hitting a magnet with installed HLS sensors, pulling or hitting the water network tubes, and creating vibrations in the HLS supporting structures, would affect measurements.

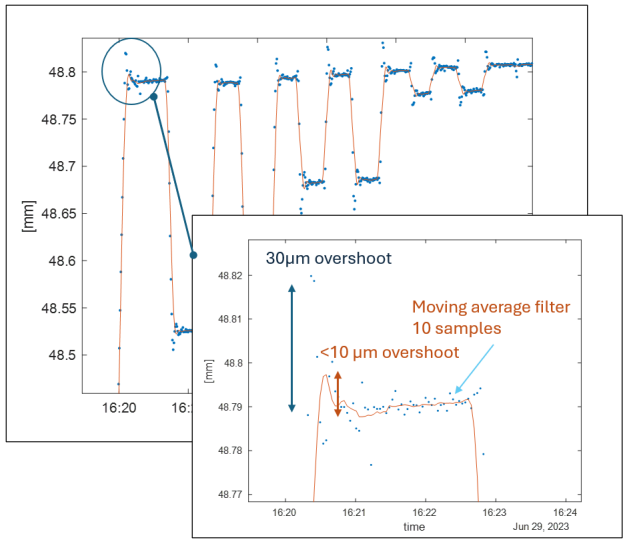

Figure 2: HLS sensor dynamic test: response to vertical TAP movements at a speed of 21 µm/s with acceleration/deceleration of 4 s.

Two tests were conducted using HLS3 (cf. Fig.1):

1. Vertical movement of the TAP up and down in steps ranging from ±0.05 to 1 mm, with a specified FRAS speed of 21 µm/s and acceleration/deceleration to nominal speed at 4 and 9 seconds.

2. Creation of a series of external disturbances to the TAP, such as hitting the magnet at various locations, striking the HLS network, squeezing flexible HLS tubes, and hitting the sensor supports.

The data acquisition sampling rate was 5 s (the only rate available at the time due to software development constraints). The output of the 10-sample moving average filter, designed for smoothing FRAS sensor data, was also tested.

Figure 2 shows part of the results from the step response test (1), conducted with a 4 s acceleration/deceleration time. For larger movements (>0.1 mm), an overshoot of approximately 30 µm is observed in the raw (blue) signal, which is expected due to the combined effect of balancing of the HLS network in transition state and to the Doppler effect on FSI measurements [13], caused by water level changes. This overshoot returns to zero after a stabilization period of 10 to 15 s, similar to the stabilization observed in LHC alignment installations with capacitive HLS sensors. Applying

the moving average filter reduces the overshoot amplitude to 10 µm. For lower acceleration/deceleration (not shown in Fig.2), the raw overshoot signal magnitude is around 10 µm and reduces to 3 µm after applying the moving average filter.

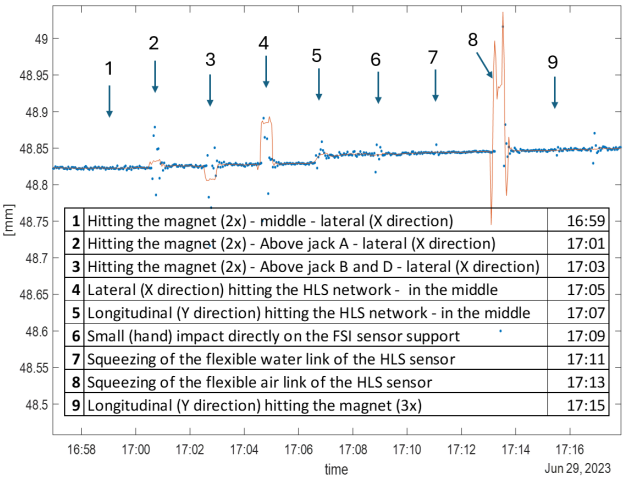

1	Hitting the magnet (2x) - middle - lateral (X direction)	16:59
2	Hitting the magnet (2x) - Above jack A - lateral (X direction)	17:01
3	Hitting the magnet (2x) - Above jack B and D - lateral (X direction)	17:03
4	Lateral (X direction) hitting the HLS network - in the middle	17:05
5	Longitudinal (Y direction) hitting the HLS network - in the middle	17:07
6	Small (hand) impact directly on the FSI sensor support	17:09
7	Squeezing of the flexible water link of the HLS sensor	17:11
8	Squeezing of the flexible air link of the HLS sensor	17:13
9	Longitudinal (Y direction) hitting the magnet (3x)	17:15

Figure 3: HLS network - sensor reaction to external disturbances

The results of the disturbance test are shown in Figure 3. Hitting the TAP magnet or sensor support at different locations (tests 1, 2, 3, 6, 9) had a small, noise-like effect on the HLS measurements, with maximum raw signal jumps of about ±80 µm.

However, hitting the mid-pillar of the HLS network tube laterally (test 4) produced a larger effect, generating raw signal perturbations up to 250 µm (peak value not shown on the graph). This may have resulted from a large lateral wave in the HLS network tube that bounced within the tube, triggering a more significant wave effect towards the sensor.

Surprisingly, altering the air pressure in the HLS sensor by squeezing the HLS connecting tube (test 8) immediately disturbed the water level in the sensor, causing signal perturbations up to 0.5 mm (raw signal samples not visible on the graph). In contrast, squeezing the water tube (test 7) did not affect the measurement. Other disturbances to the water network (tests 5, 6) caused perturbations under 20 µm.

Motorized jacks - real operation test

The SCT mock-up was crucial for the final validation of the motorized adapters and supporting jacks under realistic operating conditions, despite multiple prior tests on dedicated benches [6]. The primary issue identified during SCT validation was the friction effect of jack D on jack B's radial adjustment (see Fig.4). In the FRAS baseline, three jacks (A, B, C) support heavy components (cf. Fig.1), each providing vertical adjustment for height (Z), roll, and pitch regulation. Jacks A and B also allow a radial adjustment (X) and a yaw regulation, while jack D, rotated 90°, enables a longitudinal (Y) adjustment using a similar mechanism.

Transversal motion of the jacks (see *Force* direction in Fig.4 - right) should be free of constraints, but tight tolerances to limit backlash caused high friction forces in jack D (in the order of 4 kN) during its radial adjustment. When attempting to adjust jack B by 100 µm, the actual displacement was only about 45 µm (cf. Fig.4 - left), due to structural deformations of the jacks and floor caused by friction forces. This issue led to an immediate modification of the jack machining tolerances to prevent such problems in the future.

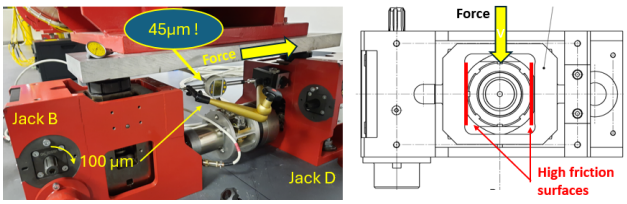

Figure 4: Left: radial motion command of Jack B by 100 µm causes only 45µm of motion; Right: Source of this issue - jack and floor deformations created by Jack D friction surfaces.

The aforementioned friction issue was detected in the frame of cycling tests of the motorized adapters and jacks, which apart from this issue showed the correct operation of the motion mechanics. The adjustment resolution in vertical and radial direction was below 1 µm. The radial motorized adapter was operational with a twice higher torque than specified. The correct operation of the motion control electronics was confirmed, with several software and electronics bugs found and corrected.

Least-squares real-time adjustment software tests

After nearly a year of SCT operation, significant progress in the development of the FRAS control software has enabled the validation of the least squares adjustment software, a core component of the FRAS control system. The least squares method is used to determine the position of all FRAS components. Given the large number of objects and configuration parameters, a generic approach was adopted using a specialized software package called LGC (*Logiciel General de Compensation*) [14, 15]. Developed at CERN, LGC was adapted to the FRAS deterministic control system by creating a dedicated DLL library package compatible with real-time FEC machines.

Figure 5 illustrates the operation of the LGC package. The LGC instance is configured with a large amount of data, including fiducialization details of aligned objects, coordinates of sensor/jack/bellows interfaces, and tunnel network parameters, all of which are used in the FRAS (SCT mock-up) least squares model. This configuration data is retrieved from multiple CERN databases and compiled into an *.xml*-like file for LGC instantiation. Once launched, LGC processes the sensor observations and all configuration parameters every second to determine the positions of all FRAS-aligned components within the tunnel's (SCT) geodetic reference frame, providing information on misalignments, required motion corrections, sensor residuals, and more.

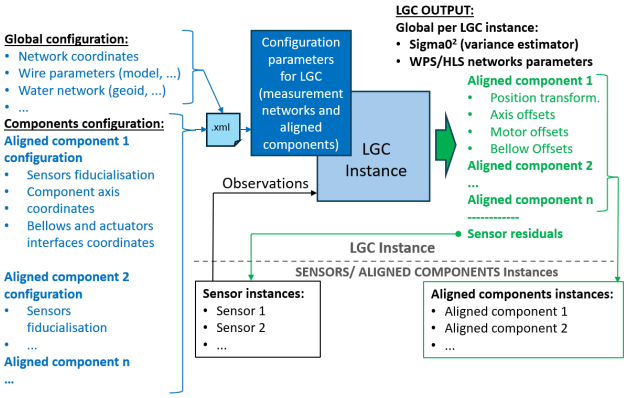

Figure 5: Schematic of LGC instance interaction with configuration and sensor observations.

To test the accuracy of LGC calculations under real conditions, the TAP magnet underwent five different motion scenarios, each representing various degrees of freedom (DOF) adjustments in the tunnel. The scenarios were:

- Radial Motion: Jacks A and B moved radially in the same direction using identical shift commands.
- Vertical Motion: Jacks A, B, and C moved vertically in the same direction using identical shift commands.
- Roll Adjustment: Jacks B and D moved vertically in opposite directions with identical shift commands, rotating the magnet around its axis, while jack A remained stationary.
- Pitch Adjustment: Jack A moved in the opposite direction to jacks B and D, which moved together using the same shift commands.
- Yaw Adjustment: Jacks A and B moved radially in opposite directions, creating rotation around the magnet's vertical axis.

For radial, vertical, yaw, and pitch adjustments, the shift commands were: 0.2, 0.2, 0.1, 0.1, 0.05, 0.02 mm. Then, following the direction change, the same steps were applied in the opposite direction to return to the initial position. For roll, smaller vertical shifts were used to avoid excessive rotation, given that jacks B and D are only 650 mm apart.

The LGC software block calculated the TAP position based on data from all installed sensors. The calculated IN and OUT coordinates of the TAP axis and roll (cf. Fig.1) were compared to the shift commands. Additionally, the accuracy of the results was verified by checking the computed sensor residuals and the least squares adjustment Sigma Zero a Posteriori ($\hat{\sigma}_0 = \sqrt{MSE}$, where MSE is the *Mean Squared Error* [16]). A $\hat{\sigma}_0$ value close to or below 1 indicates good fit quality in the least squares estimation. Higher $\hat{\sigma}_0$ values suggest that the residuals exceed the expected measurement precision, indicating a poor fit.

Figure 6.a presents example results from radial motion tests and pitch adjustments. The IN, OUT, and roll values are shown relative to their initial values (set to 0 at the start) to detect any backlash or hysteresis effects, where ideally, the magnet should return to its original position after the test. Throughout the test, the $\hat{\sigma}_0$ value remained below 0.45, indicating a good fit. All WPS sensor residuals were under 10 µm, and HLS sensor residuals did not exceed 15 µm. However, friction (hysteresis) in the double jacks was evident: the OUT coordinate of the magnet did not fully return to its initial position, showing an X shift of -0.2 mm. The remaining IN and OUT coordinates in the vertical (Z) direction and roll showed minimal change compared to the pre-test state.

Similar results were obtained for vertical, roll, and yaw adjustments, confirming the proper functioning of the acquisition systems, sensors, and LGC calculations. In the yaw adjustment test, which involved radial shifts in jacks B and D, a hysteresis effect caused by friction was again visible in the OUT radial measurements, highlighting the double jack issue. During the pitch adjustment test (shown in Fig. 6.b), a secondary effect of the longitudinal water flow in the HLS network was observed: at the start of the test $\hat{\sigma}_0$ spiked to around 4, with sensor residuals reaching nearly 150 µm. This effect is due to the slower stabilization of the HLS sensor network when larger amounts of water need to flow. Once the shifts stopped, the network required about a minute to stabilize, providing important feedback for future FRAS operations involving pitch adjustments.

An interesting effect was also noted in Fig. 6.b (top graph), where radial shift peaks of the magnet in IN and OUT were visible. These radial peaks occurred when the vertical shifts of jacks B and D were initiated non-synchronously (with a jitter of several seconds between commands). This caused a secondary roll effect on the magnet, seen as variations in the radial position peaks, as the magnet axis is 0.4 m above the jack support interfaces.

CONCLUSION

Since its deployment in June 2023, the SCT mock-up has proven to be highly valuable for finalizing improvements to the FRAS subsystems, including sensor hardware, electronics, and software. Testing on the small scale of the SCT will save significant time, costs, and efforts in future FRAS commissioning. Many hardware and procedural issues were resolved before the final procurement of the series equipment, reducing the need for last-minute on-site adjustments. Feedback on the dynamic behaviour of FRAS subsystems has enhanced the control system and shaped future operational procedures, such as managing delays in the response time linked to the inertia of the HLS network. Importantly, the main FRAS sub-components have been qualified and validated, providing essential feedback for final production.

The SCT mock-up continues to serve as the primary rehearsal platform for finalizing the control system and conducting final checks on updated equipment. It shortly be complemented by the IT String test platform.

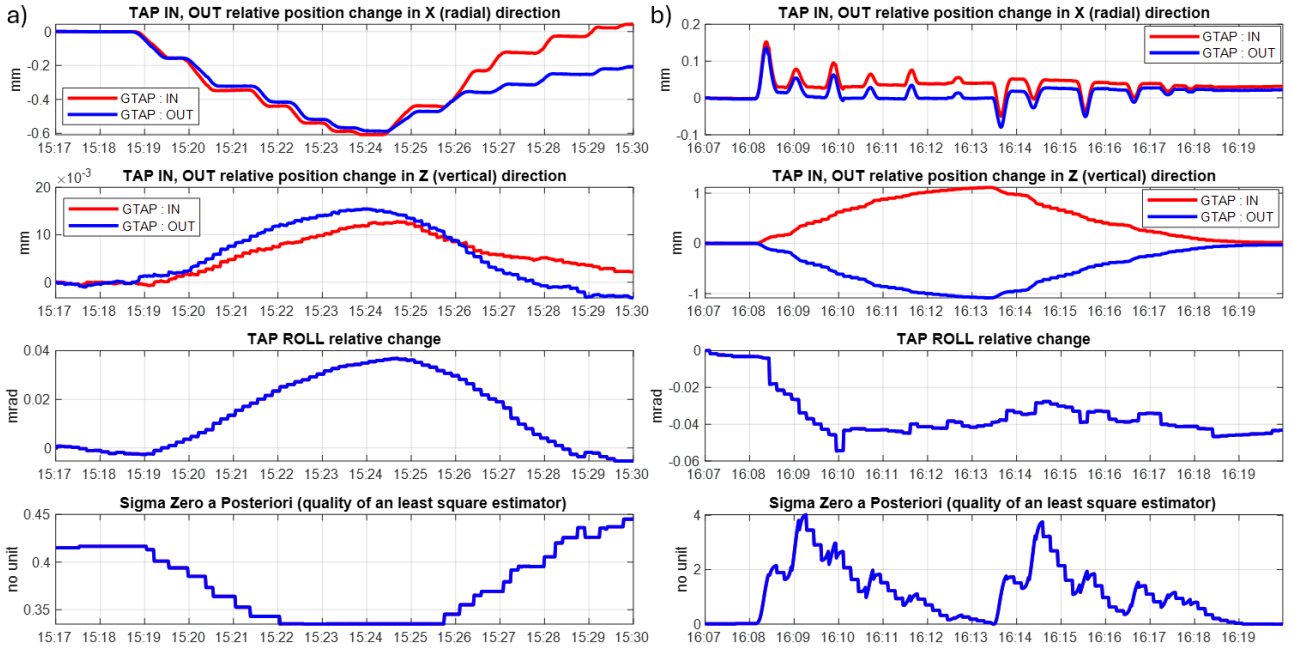

Figure 6: Example of radial and pitch motion test: a) Radial motion→ jacks A and B moved same way radially in steps: -0.2, - 0.2, -0.1, -0.1, -0.05, -0.02 mm → (direction change) → 0.2, 0.2, 0.1, 0.1, 0.05, 0.02 mm; b) Pitch motion (only vertical movements of the jacks): jack A moved in opposite steps direction than jacks B and C, which are moved in the same way: -0.2, - 0.2, -0.1, -0.1, -0.05, -0.02 mm → (direction change) → 0.2, 0.2, 0.1, 0.1, 0.05, 0.02 mm.

The SCT's life is foreseen to extend beyond the deployment of the HL-LHC FRAS, as it is planned to be used as a training platform for future FRAS users and as a test bench for system updates over an extended period.

ACKNOWLEDGEMENTS

The authors wish to thank everyone involved in this work and especially the members of three groups at CERN in the Beams Department: the Geodetic Metrology group, the Controls Electronics and Mechatronics group and the Industrial Control Systems group.

REFERENCES

[1] I. Bejar Alonso et al., "High-Luminosity Large Hadron Collider (HL-LHC) technical design report"; CERN Yellow Reports: Monographs, CERN-2020-010, CERN, Geneva, 2020, https://doi.org/10.23731/CYRM-2020-0010.

[2] V. Barbarroux et al., "Full Remote Alignment System, Engineering specification", CERN reference: LHC_-ES0049, CERN, Geneva, 2024.

[3] P. Biedrawa et al., "Full Remote Alignment System for the High-Luminosity Large Hadron Collider HL-LHC", International Workshop on Accelerator Alignment (IWAA 2022), Ferney, France, Tech. Rep. CERN-BE-2023-007, 2022, https://cds.cern.ch/record/2849056/files/CERN-BE-2023-007.pdf

[4] M. Sosin et al., "Frequency sweeping interferometry for robust and reliable distance measurements in harsh accelerator environment", Proc. SPIE 11102, 3 September 2019.

[5] M. Sosin et al., "Robust Optical Instrumentation for Accelerator Alignment Using Frequency Scanning Interferometry", 12th International Particle Accelerator Conference (IPAC2021), Campinas, Brazil, 2021, https://jacow.org/ipac2021/papers/tupab307.pdf.

[6] M. Noir et al., "Development and qualification of micrometer resolution motorized actuators for the HL-LHC collider full remote alignment system", Proc. 12th Int. Conf. Mech. Eng. Design Synchrotron Radiat. Equip. Instrum. (MEDSI'23), Beijing, China, 2023, https://jacow.org/medsi2023/papers/thoam01.pdf.

[7] M. Arruat et al., "Front-End Software architecture", Proc. of International Conference on Acceleratorand Large Experimental Physics Control Systems (ICALEPS07), 15-19 October 2007, Knoxville, Tennessee, USA.

[8] https://unicos.web.cern.ch/

[9] A. Masi, P. Peronnard, "High performance field Sensors Acquisition and Motion Control system (SAMbuCa) for future critical missions in EN-SMM", EDMS 2274146, CERN, 2019.

[10] B. Fernandez Adiego et al., "Protection layers design for the High Luminosity LHC Full Remote Alignment System", 19th International Conference on Accelerator and Large Experimental Physics Control Systems (ICALEPS 2023), Cape Town, South Africa, 7-13 Oct 2023.

[11] M. Sosin, "Functional specification. Full Remote Alignment system – Software", EDMS 2589302, CERN, 2022.

[12] https://nxcals-docs.web.cern.ch/current/

[13] M. Sosin et al., Impact of vibrations and reflector movements on the measurement uncertainty of Fourier-based Frequency

Sweeping Interferometry, Proc. SPIE, San Francisco, California, United States, 2020, https://doi.org/10.1117/12.2560998

[14] M. Jones, M. Barbier,T. Hubinek, Mathematical Survey Observation Model for LGC2, EDMS 146553, CERN, Geneva, 2015.

[15] G. Kautzmann, J. Gutekunst, F. Klumb, LGC open source: a strategy to share adjustment software and algorithmic development, this conference.

[16] Mean Squared Error. In: The Concise Encyclopedia of Statistics. Springer, New York, NY, 2008, https://doi.org/10.1007/978-0-387-32833-1_251.